Transition to oscillatory natural convection of water near its density maximum in a tall enclosure

Assessment of three-dimensional effects

C.J. Ho and F.J. Tu
Department of Mechanical Engineering, National Cheng Kung University, Tainan, Taiwan, Republic of China

Keywords *Convection, Simulation, Water*

Abstract *Numerical simulations have been performed for three-dimensional natural convection of water near its maximum-density (cold water) inside rectangular enclosures with differential heating at the vertical (left and right) walls. The horizontal (top and bottom) walls and the lateral (front and rear) walls are taken as insulated. Computations are performed for the buoyancy-driven convection of cold water with density inversion parameter $\theta_m = 0.5$ in the enclosures with aspect ratio (height/width) $A_y = 8$ and depth ratios (depth/width) $A_z = 0.5$, 1, and 2. The influence of the depth ratio on the onset of oscillatory convection in a cold-water-filled enclosure is investigated. The presence of the lateral walls tends to suppress the onset of unsteadiness in the convective flow. The main features of the oscillatory convection flow and temperature fields as well as the instability mechanism in the three-dimensional enclosure were similar to those found in the two-dimensional model. However, there exists a strong three-dimensionality in the spatial distribution of the fluctuation amplitude. With the decrease of the depth ratio, the damping effect of the lateral walls becomes increasingly pronounced, leading to a reduced heat transfer rate.*

Nomenclature

A_y = aspect ratio, H/W
A_z = depth ratio, D/W
b = exponent in the density equation
D = depth
f^+ = frequency
f = dimensionless frequency, f^+W^2/α
Fo = Fourier number, $\alpha t/W^2$
g = gravitational acceleration
H = height
Pr = Prandtl number, ν/α
Ra = Rayleigh number based on width, $g \cdot rsp(\Delta T)^b W^3/(\nu\alpha)$
Ra_H = Rayleigh number based on height, $g \cdot rsp(\Delta T)^b H^3/(\nu\alpha)$
rsp = coefficient in density equation
t = time
T = temperature
ΔT = temperature difference between hot and cold wall, $(T_h - T_c)$
u_i, u_j = velocity components
$\mathbf{V}$ = dimensionless velocity vector
W = width
x^+, y^+, z^+ = Cartesian coordinates

Support for this study by the National Science Council of the Republic of China in Taiwan through Project Nos. NSC-83-221-E006-110 and NSC-84-2212-E006-013 is gratefully acknowledged. The necessary computing resources are kindly provided by the National Center for High Performance Computing of NSC. The constructive comments of the reviewers are sincerely appreciated.

International Journal of Numerical Methods for Heat & Fluid Flow, Vol. 11 No. 7, 2001, pp. 626-641.

x, y, z = dimensionless coordinates, $x^+/W, y^+/W, z^+/W$

Greek symbols

α = thermal diffusivity

θ = dimensionless temperature, $(T - T_c)/\Delta T$

θ_m = density inversion parameter, $(T_m - T_c)/\Delta T$

ν = kinematic viscosity

ρ = density

$\tilde{\omega}$ = dimensionless pseudovorticity vector

Superscripts

$-$ = time-averaged value

$'$ = fluctuating component

Subscripts

c = cold wall

cr = critical state

h = hot wall

m = maximum density, or periodically mean value

Introduction

For the past decades, there have been a number of studies of the natural convection of water near its density maximum (cold water) inside a vertical rectangular enclosure with differentially heated sidewalls. Cold water is known to feature an anomalous density-temperature relationship, the so-called density inversion phenomenon, having its maximum density at about 4°C at the sea-level atmospheric pressure. The representative works for steady-state (Seki *et al.*, 1978; Lin and Nansteel, 1987; Tong and Koster, 1993) and transient (Vasseur and Robillard, 1980; Braga and Viskanta, 1992) natural convection in vertical rectangular enclosures filled with cold water revealed that the buoyancy-driven flow structure and heat transfer are strongly affected by the density inversion phenomenon, giving rise to some interesting phenomena such as multicellular flows and heat transfer extremes.

Recently, the interest of study has turned to the transition into oscillatory convection that occurs when the Rayleigh number is increased to sufficiently large values. Nishimura *et al.* (1995) undertook a numerical investigation concerning the occurrence of oscillatory natural convection of cold water in a vertical rectangular enclosure of aspect ratio 1.25 at the Rayleigh numbers of $10^5 \sim 10^8$. Their simulations failed to predict unstable buoyant flow and temperature fields in the enclosure. Nishimura and his co-workers (1997) further examined experimentally and numerically the effect of initial temperature on the inception of oscillatory natural convection of cold water in a vertical enclosure of aspect ratio 1.25. The vertical walls of the enclosure were maintained isothermal, respectively, at 8°C and 0°C. With the initial temperature at 4°C, an unstable buoyant flow in the enclosure was observed for $Ra_H > 9 \times 10^6$, featuring an oscillatory sinking jet-like flow structure. At an initial temperature other than 4°C, however, no oscillatory flow was detected experimentally. In the corresponding finite-element simulations, only partial agreement was found in comparison with the experimental results. Recently, the present authors presented a numerical study (Ho and Tu, 1999) concerning the inception of oscillatory natural convection of cold water in a two-dimensional vertical enclosure of high aspect ratio ($A_y = 8$). With incremental increase in the Rayleigh number, transition into self-sustained oscillatory convection regime in the cold-water-filled enclosure through a Hopf bifurcation

was predicted. An oscillatory multicellular structure prevails within counter-rotating bicellular flow regions, featuring a traveling wave motion of the maximum density contour of water. The nature of the transitional instability into oscillatory convection in the tall enclosure was demonstrated to be buoyancy-driven. The critical Rayleigh numbers for the transition into oscillatory convection were found to be $4 \times 10^5 < Ra_{cr} < 5 \times 10^5$ and $7 \times 10^4 < Ra_{cr} < 8 \times 10^4$ for the density inversion parameter $\theta_m = 0.4$ and 0.5, respectively. In a similar geometry but under the initial cold-start conditions, occurrence of the oscillatory convection was visualized experimentally in a more recent study of transient natural convection of cold water (Ho and Tu, 2001). However, there exist substantial discrepancies between the two- and three-dimensional numerical simulations corresponding to the experiments, reflecting significant three-dimensional effects on the transition process.

The present study aims, accordingly, to assess numerically the three-dimensional effects on transition to oscillatory convection of cold water in the physical configuration considered in the previous study (Ho and Tu, 1999).

Numerical formulation

Figure 1 displays a schematic of the simulated configuration of a rectangular enclosure of dimensions $W \times H \times D$ filled with water near its density maximum. The left-hand vertical wall is isothermally heated at a constant temperature T_h; while the right-hand vertical wall remains isothermal at a constant temperature T_c ($< T_h$). The remaining sidewalls of the enclosure are taken as adiabatic.

Governing equations

The governing equations for the three-dimensional transient laminar natural convection in the cold-water-filled enclosure are formulated adopting the pseudovorticity-velocity formulation (Ho and Lin, 1997). Physical properties of water, except for the density in the buoyancy force terms, are assumed constant. The non-dimensional governing equations in terms of the

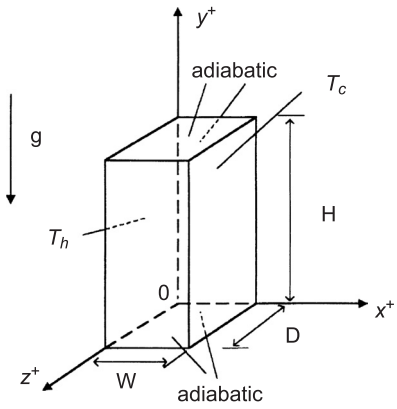

Figure 1.
Schematic diagram of the physical configuration and coordinate systems

pseudovorticity vector $\tilde{\omega}$, velocity vector $\mathbf{V}$ and temperature θ can be expressed as follows:

$$\frac{\partial \mathbf{V}}{\partial Fo} + \nabla \times (\tilde{\omega} + \mathrm{Pr}\nabla \times \mathbf{V}) = 0 \tag{1}$$

$$\nabla^2 \tilde{\omega} = \nabla \times [\mathbf{V} \times (\nabla \times \mathbf{V})] + \mathrm{Pr}Ra\nabla \times (|\theta - \theta_m|^b \hat{\mathbf{e}}_g) \tag{2}$$

$$\frac{\partial \theta}{\partial Fo} + \mathbf{V} \cdot \nabla\theta = \nabla^2\theta \tag{3}$$

Here, the following density-temperature correlation (Gebhart and Mollendorf, 1974) was used for evaluating the density of the cold water:

$$\rho = \rho_m(1 - rsp|T - T_m|^b) \tag{4}$$

where ρ_m = 999.9720kg/m^3, rsp = 9.297173 × 10^{-6}(°C)$^{-b}$, b = 1.894816, and T_m = 4.029325°C.

The boundary conditions at the enclosure walls are:

$$x = 0; \quad \mathbf{V} = \mathbf{0}, \theta = 1 \tag{5a}$$

$$x = 1; \quad \mathbf{V} = \mathbf{0}, \theta = 0 \tag{5b}$$

$$y = 0 \text{ and } A_y; \quad \mathbf{V} = \mathbf{0}, \partial\theta/\partial y = 0 \tag{5c}$$

$$z = 0 \text{ and } A_z; \quad \mathbf{V} = \mathbf{0}, \partial\theta/\partial z = 0 \tag{5d}$$

The boundary conditions for the pseudovorticity on the sidewalls of the enclosure can be evaluated explicitly from the wall vorticity (Ho and Lin, 1997). As the initial condition, we take a solution obtained for a lower Rayleigh number.

The foregoing formulation clearly reveals that the relevant dimensionless parameters for the three-dimensional natural convection in the cold-water-filled enclosure include: the Rayleigh number, Ra; the Prandtl number, Pr; the density inversion parameter, θ_m; the aspect ratio (height/width), A_y; and the depth ratio (depth/width), A_z. The density inversion parameter θ_m, as shown in the earlier studies (Lin and Nansteel, 1987; Ho and Tu, 1999), essentially controls the orientation of the maximum density temperature T_m with respect to the vertical wall temperatures T_h and T_c and has a fundamental effect on the flow structure and heat transfer in the enclosure.

Method of solution

The differential equations were discretized spatially using a second-order central difference approximation for the diffusion terms and the QUICK scheme

(Leonard, 1983) for the advection terms. A non-uniform grid in the x-direction was constructed for effectively capturing the steep gradients along the thermally active walls of the enclosure, while uniform grids were used in both y- and z-directions. The time-dependent velocity and temperature Equations (1) and (3) were integrated in time using an explicit approximation with second-order accuracy.

Based on the results of the previously obtained solution of the approximate value of the Rayleigh number as the initial condition, the simulation starts with solving equations (1) and (3) for the velocity and temperature fields, respectively. A time step of 5×10^{-6} was found sufficiently small for the present simulations. At each time step, the discretized pseudovorticity equation (2) is calculated iteratively by a successive relaxation method until a relative convergence criterion of less than 5×10^{-7} is met. The transient solution is considered asymptotically approaching a steady state condition, if the relative convergence criteria of 10^{-7} and 5×10^{-7} are, respectively, satisfied for the solutions of temperature and velocity.

Throughout the present simulations, double-precision arithmetic was incorporated to achieve high solution accuracy. Based on a grid-size variation study, a grid of $37 \times 201 \times 31$ ($x \times y \times z$) was found to be sufficiently fine for the simulations. CPU times required for a calculation on an IBM SP2 workstation range from 290 to 400 hours, depending on the Rayleigh number and the occurrence of the oscillatory convection.

The present three-dimensional code was validated obtaining excellent agreement with the reported solutions for steady state natural convection in an air-filled cubic enclosure (Le Peutrec and Lauriat, 1990; Fusegi *et al.*, 1991), as demonstrated by the comparison of the surface-averaged Nusselt number at various Rayleigh numbers shown in Table I.

Results and discussion

In the present work, the aspect ratio of the enclosure, A_y, was fixed at eight. Three values of the depth ratio, $A_z = 0.5$, 1, and 2, were considered to unveil possible effects of the lateral (front and rear) vertical walls on transient convection of cold water in the enclosure. The simulations were undertaken by varying Rayleigh number under the condition of $\theta_m = 0.5$.

Table I.
Comparison of results for natural convection in an air-filled cubic enclosure

	$\overline{Nu}$		
Ra	Le Peutrec and Lauriat (1990)	Fusegi *et al.* (1991)	Present simulation
10^3	–	1.085	1.057
10^4	–	2.100	2.074
10^5	4.348	4.361	4.367
10^6	8.651	8.770	8.755

Steady state convection

In the enclosure of $A_z = 2$, steady state convection was found to reach asymptotically for $Ra = 10^4 \sim 9 \times 10^4$. The three-dimensionality of the buoyancy-driven flow structure and temperature field can be qualitatively inferred from the disparity among the plots of velocity vector and isotherm at three *x-y* planes shown in Figure 2 for $Ra = 9 \times 10^4$. The velocity vector plots were scaled with the maximum velocity in the cross-section of interest. Under the influence of the density inversion, a bicellular flow structure with a downward stream along the maximum density contour of water is clearly formed at each *x-y* cross-section. The symmetry of the cross-sectional velocity and temperature fields with respect to the mid-plane $z = 1$ can be readily detected from Figure 2.

Transition to oscillatory convection

As the Rayleigh number is further increased to 10^5, a self-sustained periodically oscillatory convection regime prevails in the enclosure of $A_z = 2$ with a dimensionless frequency of $f = 47.4$, which is very close to the value of 47.2 predicted in the corresponding two-dimensional simulation (i.e. $A_z = \infty$) (Ho and Tu, 1999). Figures 3 and 4 display, respectively, a time sequence of the cross-sectional velocity field and temperature distribution in two *x-y* planes over one period of oscillation. In the mid-plane $z = 1$, the cyclic sequence of unsteady multicellular flow development (Figure 3(ii)) synchronized with the upward-traveling wavy temperature variation (Figure 4(ii)) is very similar to that found in the two-dimensional model. On approaching the rear lateral wall at $z = 0.133$ (Figures 3(i) and 4(i)), the cyclic variation of the cross-sectional

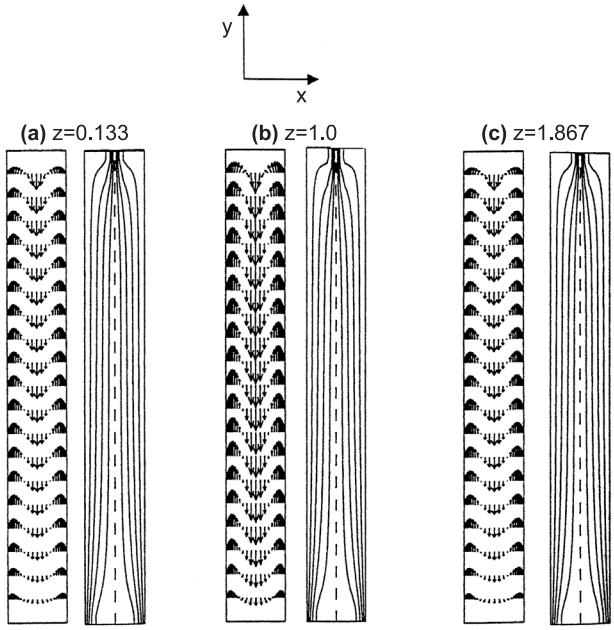

Figure 2.
Steady state cross-sectional velocity vectors (right) and isotherms (left) in selected *x-y* planes with $A_z = 2$ at $Ra = 9 \times 10^4$

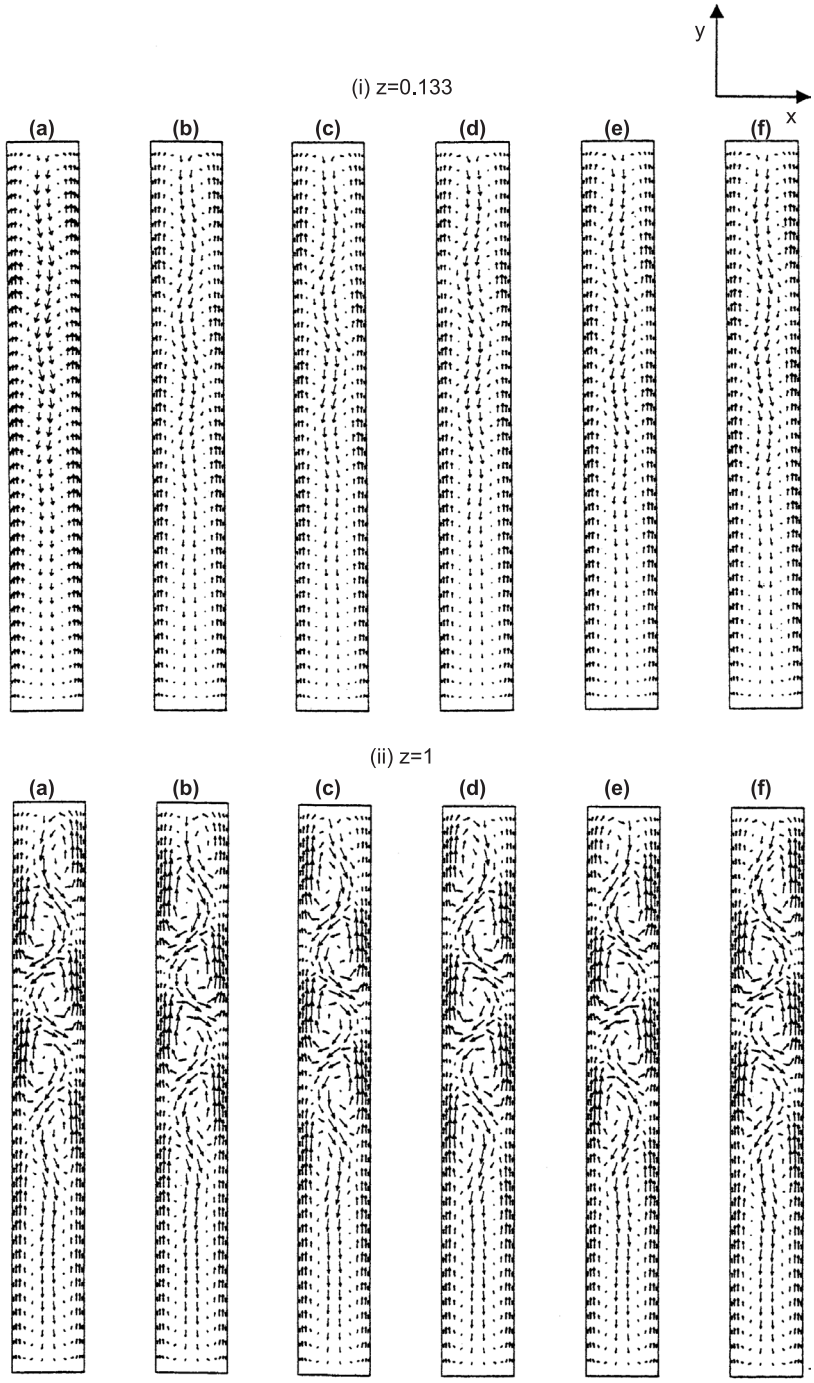

Figure 3.
Cyclic variation of cross-sectional (*x-y* plane) velocity vectors at (i) $z = 0.133$ and (ii) $z = 1$ with $A_z = 2$ and $Ra = 10^5$

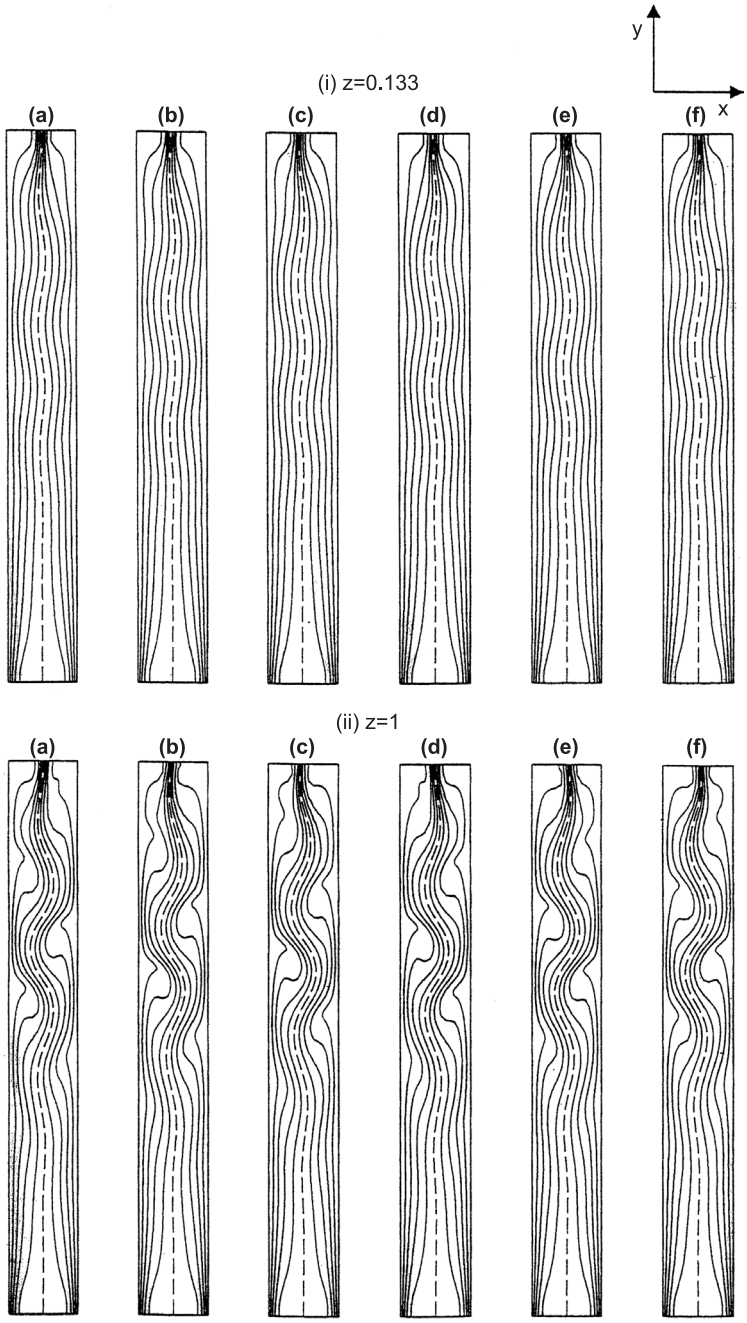

Figure 4.
Cyclic variation of cross-sectional (x-y plane) isotherms at (i) $z = 0.133$ and (ii) $z = 1$ with $A_z = 2$ at $Ra = 10^5$

velocity and temperature fields can be seen to be similar to those in the midplane $z = 1$ but with greatly subdued unsteadiness, reflecting the effect of viscous dissipation by the presence of the lateral walls in the three-dimensional enclosure. The maximum density jet flow coming off the midpoint of the ceiling, as shown in Figure 3(i), is substantially weaker with the minute vortex-splitting phenomenon occurring only in the upper-half central core region of the enclosure. The foregoing suggests that the instability mechanism in the three-dimensional enclosure is similar to that observed in the two-dimensional model. The two-dimensional nature of the oscillatory flow can be further demonstrated by the cyclic variation of the cross-sectional velocity structures at three *x-z* planes ($y = 2$, 4, and 6) shown in Figure 5 under the same conditions as Figures 3 and 4. The cross-sectional flow structures at various horizontal planes oscillate mainly along the *x* direction, displaying more or less symmetry with respect to the *x-y* mid-plane $z = 1$.

Figure 6 presents the contour lines of equal amplitude of the temperature fluctuations in the *x-y* planes of $z = 0.133$ and 1 inside the enclosure of $A_z = 2$ for $Ra = 10^5$. The amplitude of temperature fluctuation was evaluated in every grid point by subtracting the local time-averaged value from the local instantaneous value. The solid and dashed contours denote, respectively, the local instantaneous temperature higher and lower than the local time-averaged temperature. Resembling the cyclic variation that was predicted in the two-dimensional model (Ho and Tu, 1999), the temperature fluctuation arises at the lower-quarter region, whereupon the maximum density contour begins its meandering; then intensifies on its course of upward drifting along the vertical central core; and finally diminishes at the ceiling of the enclosure. Comparison of the fluctuation structures in two *x-y* planes of $z = 1$ and 0.133, shown in Figure 6, indicates that the temperature fluctuation amplitude has a distinct structure as a function of the depth *z*. In the plane near the rear lateral wall $z = 0.133$, the amplitude of temperature fluctuation appears to be substantially suppressed due to the presence of the lateral wall in the three-dimensional enclosure. Moreover, the three-dimensional oscillatory convection exhibits a symmetric temperature fluctuation structure with respect to *x-y* mid-plane ($z = 1$) of the enclosure, as can be inferred from the cyclic variations of the temperature fluctuation in different *x-z* planes displayed in Figure 7.

Further, the nature of the instability mechanisms for the present case is examined by evaluating the production of the fluctuating kinetic energy of the oscillatory convection like that performed in the previous two-dimensional simulation (Ho and Tu, 1999). The resultant distributions of local production of time-averaged fluctuating kinetic energy due to flow shear and buoyancy in two *x-y* planes of the enclosure are, respectively, presented in Figure 8. The local production of fluctuating kinetic energy due to the shear of the mean flow and the buoyancy forces are defined as $-u_i'u_j' \, \partial\overline{u_i}/\partial x/_j$ and $Ra \, \mathrm{Pr} \, [2(\overline{\theta} - \theta_m)\theta' + (\theta')^2]\partial_{i2}$, respectively. It can be seen that in the *x-y* mid-plane ($z = 1$) the buoyancy is the dominant source for the production of the fluctuating kinetic energy with a spatial distribution occupying the upper

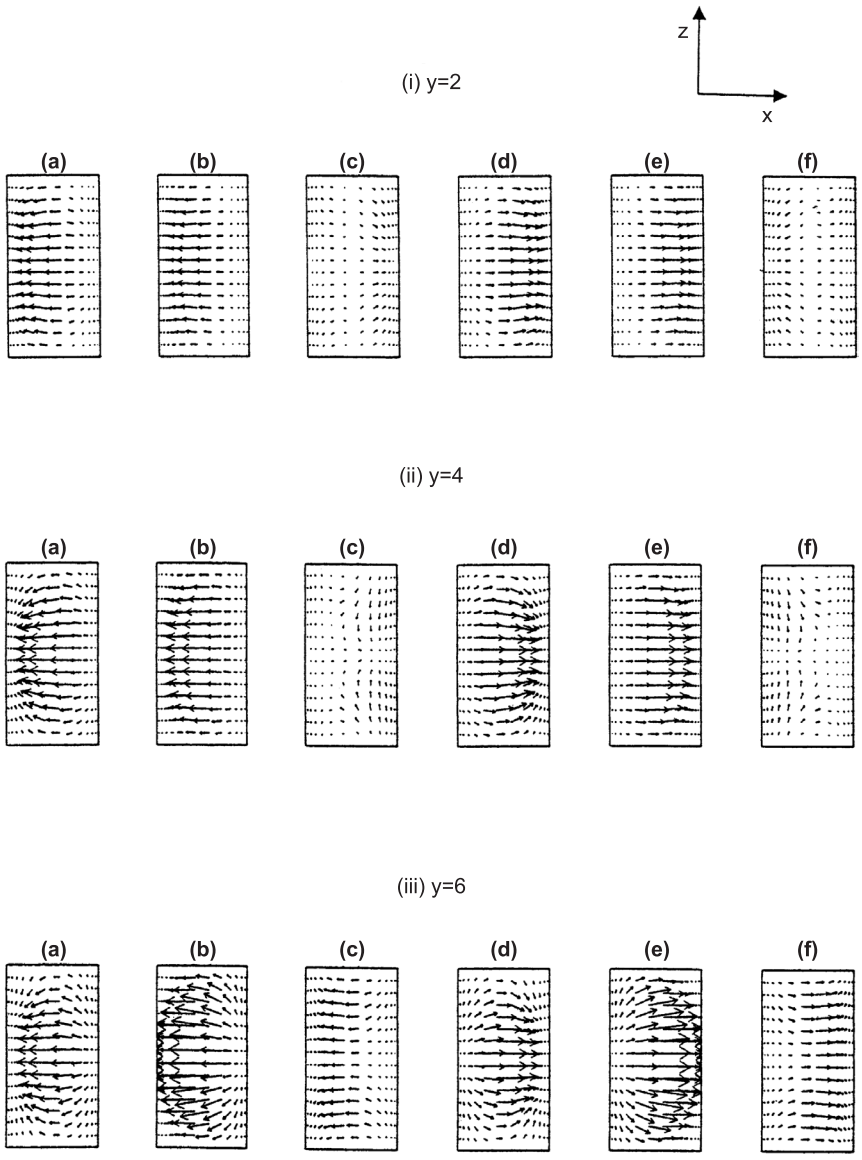

Figure 5.
Cyclic variation of cross-sectional (x-z plane) velocity vectors at (i) y = 2, (ii) y = 4, and (iii) y = 6 for $Ra = 10^5$ with $A_z = 2$.

two-thirds portion of the enclosure. Moving toward the lateral wall, the contribution of the buoyancy or the flow shear to the production of the fluctuating kinetic energy is markedly reduced, as exemplified by Figure 8(i) for the plane $z = 0.133$. Further, the buoyancy is found to be the sole source for the total production of the fluctuating kinetic energy in the three-dimensional enclosure, similar to that found in the two-dimensional model. The instability mechanism for the transition into oscillatory convection inside the three-dimensional cold-water-filled enclosure is therefore thermal in nature.

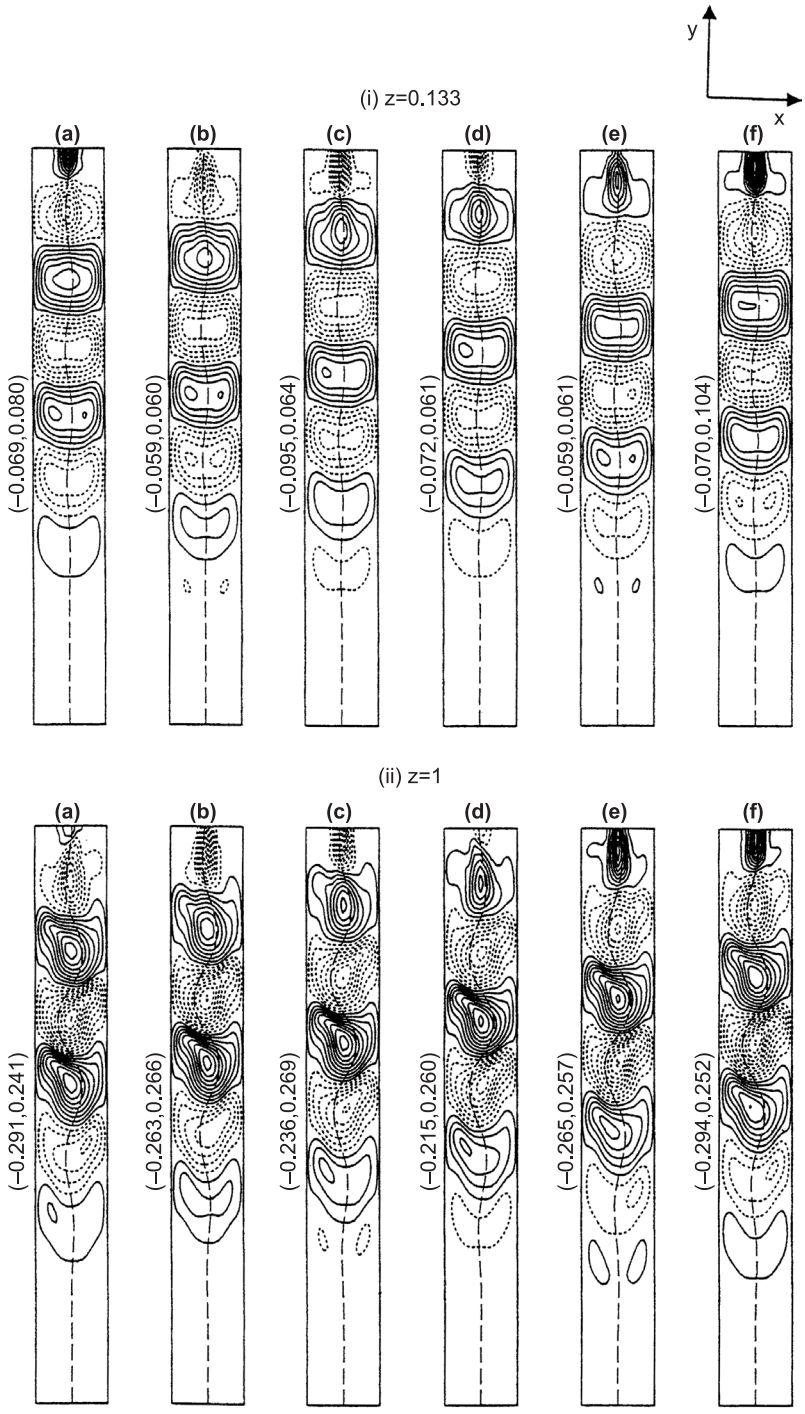

Figure 6.
Cyclic variation of amplitude of the temperature oscillations in the *x-y* plane at (i) $z = 0.133$ and (ii) $z = 1$ with $A_z = 2$ at $Ra = 10^5$

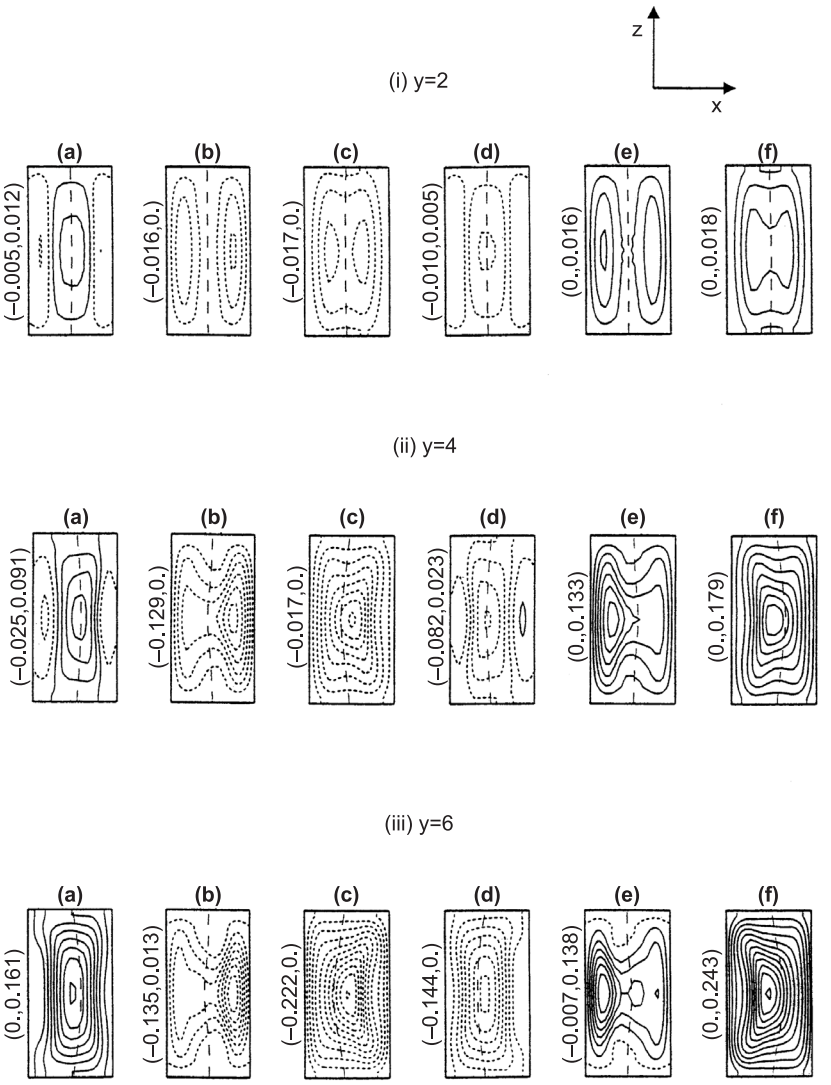

Figure 7.
Cyclic variation of amplitude of the temperature oscillations in the x-z plane at (i) $y = 2$, (ii) $y = 4$, and (iii) $y = 6$ with $A_z = 2$ at $Ra = 10^5$

Supercritical simulations for the enclosure of $A_z = 2$ were further carried out by progressive increase of the Rayleigh number up to 1.2×10^5. The solutions to these cases all remain periodic at increasingly higher frequencies. The critical Rayleigh number for the transition into oscillatory convection for the three-dimensional enclosure of $A_z = 2$ is thus estimated to be between 9×10^4 and 10^5, which is about 12 per cent higher than that found in the two-dimensional enclosure (Ho and Tu, 1999). This clearly reflects that the presence of the lateral walls exerts a damping effect on the inception of the oscillatory convection in the three-dimensional enclosure.

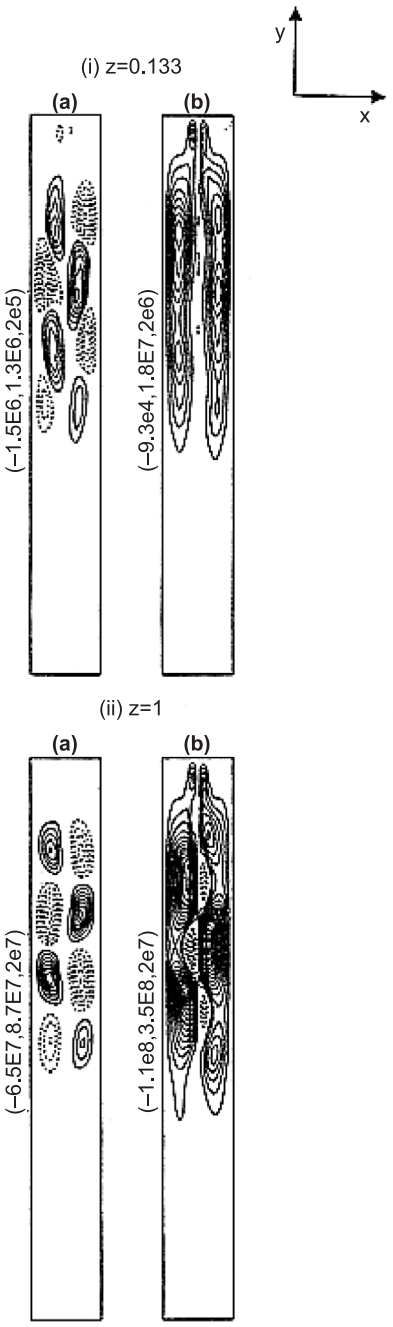

Figure 8.
Cross-sectional distributions of local production of time-integrated fluctuating kinetic energy due to (a) flow shear and (b) buoyancy in two *x-y* planes with $A_z = 2$ at $Ra = 10^5$. Negative iso-values are denoted by dotted lines

To further unveil the influence of the lateral wall, simulations were undertaken for the enclosure of the depth ratio $A_z = 1$ and 0.5 by progressively increasing the Rayleigh number up to 4×10^5 and 5×10^5, respectively. All the simulations were found reaching steady state flow field and temperature distribution, a further indication of the damping effect due to the presence of the lateral walls. This finding is consistent with that found for the air-filled enclosure (Janssen *et al.*, 1993). Figure 9 exemplifies the steady state cross-sectional distribution of isotherms and velocity vectors in the enclosure of $A_z = 1$ at $Ra = 4 \times 10^5$. In the planes near the lateral walls ($z = 0.1$ and 0.9), the buoyancy-driven flow is clearly weaker than that in the x-y mid-plane ($z = 0.5$) of the enclosure.

Finally, results of the surface-averaged heat flux for the steady state or periodically oscillatory convection in the cold-water-filled enclosure are presented by plotting the time- and surface-averaged Nusselt number along the hot wall, $\overline{Nu}_{h,m}$, versus the Rayleigh number, as shown in Figure 10. Also included in Figure 10 are the data obtained from the two-dimensional simulations, which can be viewed as $A_z = \infty$. It is evident from the plot that the heat transfer rate has a strong bearing with the depth ratio, A_z, of the enclosure. At a fixed Rayleigh number, the decrease of the depth ratio leads to a significant decrease of the heat transfer rate across the enclosure, signifying further the damping effect of the lateral walls. Further examination of Figure 10 reveals that, in the oscillatory convection regime, the heat transfer rate exhibits a sharper increase with the Rayleigh number.

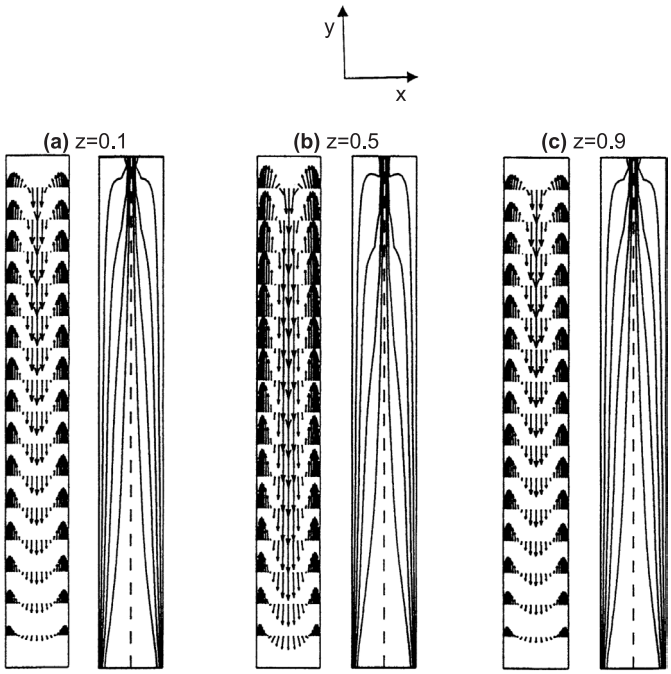

Figure 9.
Steady state cross-sectional isotherms (right) and velocity vectors (left) in selected x-y planes with $A_z = 1$ at $Ra = 4 \times 10^5$

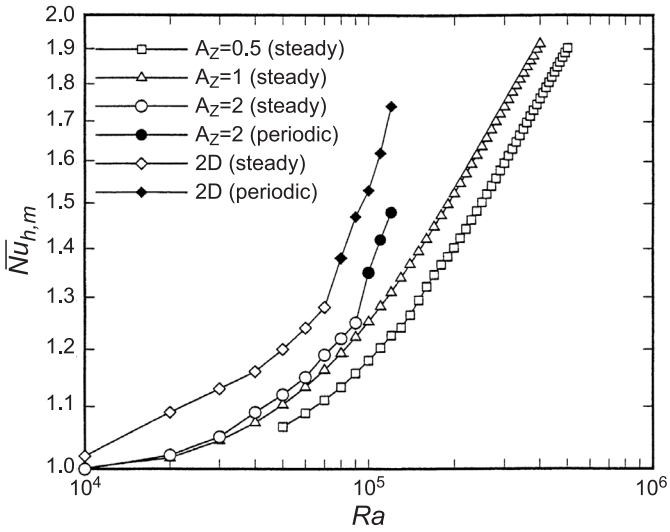

Figure 10.
Variation of time- and surface-averaged heat transfer rate across the enclosure with the Rayleigh number

Concluding remarks

In the present study, three-dimensional numerical simulation has been performed to assess the three-dimensional effects on inception of oscillatory natural convection in a vertical high-aspect-ratio ($A_y = 8$) enclosure filled with cold water. Comparisons between results were made for $\theta_m = 0.5, 10^4 \leq Ra \leq 5 \times 10^5, A_z = 0.5, 1, 2,$ and ∞ (two-dimensional model).

Overall, the three-dimensional predictions in the main features of the oscillatory convection flow and temperature fields as well as the instability mechanism were similar to those found in the two-dimensional model. However, there exists a strong three-dimensionality of the oscillatory flow and temperature fields in the enclosure. The oscillatory convection has a significant effect on heat transfer rate across the enclosure. The three-dimensional convection in the cold-water enclosure can be strongly affected by the depth ratio A_z of the enclosure due to the presence of the lateral walls. The viscous damping associated with the presence of the lateral walls tends to suppress the unsteadiness of three-dimensional convection and hence the heat transfer rate inside the enclosure.

References and further reading

Braga, S.L. and Viskanta, R. (1992), "Transient natural convection of water near its density extremum in a rectangular cavity", *Int. J. Heat Mass Transfer*, Vol. 35, pp. 861-75.

Fusegi, T., Hyun, J., Kuwahara, M.K. and Farouk, B. (1991), "A numerical study of three-dimensional natural convection in a differential heat cubical enclosure", *Int. J. Heat Mass Transfer*, Vol. 34, pp. 1543-57.

Gebhart, B. and Mollendorf, J. (1974), "A new density relation for pure and saline water", *Deep Sea Research*, Vol. 24, pp. 831-8.

Ho, C.J. and Lin, F.H. (1997), "Simulation of natural convection in a vertical enclosure by using a new incompressible flow formulation – pseudovorticity-velocity formulation", *Numerical Heat Transfer*, Part A, Vol. 31, pp. 881-96.

Ho, C.J. and Tu, F.J. (1999), "Numerical study on oscillatory convection of cold water in a tall vertical enclosure", *Int. J. Numerical Methods for Heat & Fluid Flow*, Vol. 9, pp. 487-508.

Ho, C.J. and Tu, F.J. (2001), "Visualization and prediction of natural convection of water near its density maximum in a tall rectangular enclosure at high Rayleigh numbers", *ASME J. Heat Transfer*, Vol. 123, pp. 84-95.

Ivey, G.N. and Hamblin, P.F. (1989), "Convection near the temperature of maximum density for high Rayleigh number, low aspect ratio, rectangular cavities", *ASME Journal of Heat Transfer*, Vol. 111, pp. 100-5.

Janssen, R.J.A., Henkes, R.A.W.M. and Hoogendoorn, C.J. (1993), "Transition to time-periodicity of a natural-convection flow in a 3-D differentially heated cavity", *Int. J. Heat Mass Transfer*, Vol. 36, pp. 2927-40.

Lankford, K.E. and Bejan, A. (1986), "Natural convection in a vertical enclosure filled with water near 4°C", *ASME Journal of Heat Transfer*, Vol. 108, pp. 755-63.

Le Peutrec, Y. and Lauriat, G. (1990), "Effects of the heat transfer at the side walls on natural convection in cavities", *ASME Journal of Heat Transfer*, Vol. 112, pp. 370-8.

Leonard, B.P. (1983), "A convectively stable, third-order accurate finite difference method for steady two-dimensional flow and heat transfer", in Shih, T.M. (Ed.), *Numerical Properties and Methodologies in Heat Transfer*, Hemisphere Publishing Corp., Washington, DC, pp. 211-26.

Lin, D.S. and Nansteel, N.W. (1987), "Natural convection heat transfer in a square enclosure containing water near its density maximum", *Int. J. Heat Mass Transfer*, Vol. 30, pp. 2319-29.

McDonough, M.W. and Faghri, A. (1994), "Experimental and numerical analyses of the natural convection of water through its density maximum in a rectangular enclosure", *Int. J. Heat Mass Transfer*, Vol. 37, pp. 783-801.

Nishimura, T., Wake, A. and Fukumori, E. (1995), "Natural convection of water near the density extremum for a wide range of Rayleigh numbers", *Numerical Heat Transfer*, Part A, Vol. 27, pp. 433-49.

Nishimura, T., Hayashida, Y., Mineoka, M. and Wake, A. (1997), "Oscillatory natural convection of water near the density extremum at high Rayleigh numbers", *Int. J. Heat Mass Transfer*, Vol. 40, pp. 3449-65.

Seki, N., Fukusako, S. and Inaba, H. (1978), "Visual observation of nature convective flow in a narrow vertical cavity", *J. Fluid Mech.*, Vol. 84, pp. 695-704.

Tong, W. and Koster, J. (1993), "Natural convection of water in a rectangular cavity including density inversion", *Int. J. Heat Fluid Flow*, Vol. 14, pp. 366-75.

Vasseur, P. and Robillard, L. (1980), "Transient natural convection heat transfer in a mass of water cooled through 4°C", *Int. J. Heat Mass Transfer*, Vol. 23, pp. 1195-205.